AIAA JOURNAL
Vol. 35, No. 3, March 1997

Thermopiezoelectric Control Design and Actuator Placement

M. Sunar*
King Fahd University of Petroleum and Minerals, Dhahran 31261, Saudi Arabia
and
S. S. Rao†
Purdue University, West Lafayette, Indiana 47907-1288

The quasistatic thermopiezoelectricity equations are used to include thermal effects in piezoelectric sensing and control systems. The finite element equations are developed for thermopiezoelectric sensor and actuator design. Static and dynamic case studies are carried out to observe the temperature effects in the piezoelectric control systems. Thermal effects are also included in the piezoelectric actuator location problem for the cantilever beamlike problems. It is found that the displacements caused by the temperature effects are important in the precision sensing and control of distributed systems by piezoelectric materials. It is also concluded that for the cantilever beamlike problems, in the presence of a uniformly distributed thermal field, the thermopiezoelectric actuators are to be located closer to the fixed end for a more effective control of structural oscillations.

Nomenclature

A	= system matrix
B	= input matrix
$C_{\theta u}$	= thermal expansion rate matrix
$C_{\theta\theta}$	= heat conduction rate matrix
$C_{\theta\phi}$	= pyroelectric rate matrix
c	= matrix of elastic stiffness coefficients
c_p	= capacitance
$\boldsymbol{D}$	= vector of charge per unit area
d	= distance of piezoelectric/thermopiezoelectric actuator pair from fixed end
$\boldsymbol{E}$	= electric field vector
e	= matrix of piezoelectric coefficients
$\boldsymbol{F}$	= global mechanical force (disturbance) vector
$\boldsymbol{G}$	= global feedback charge vector
h	= height
$\boldsymbol{h}$	= vector of heat flux
I	= moment of inertia
J	= performance index
K	= matrix of heat conduction coefficients
K_G	= constant gain matrix
K_{uu}	= elastic stiffness matrix
$K_{u\theta}$	= thermal expansion stiffness matrix
$K_{u\phi}$	= piezoelectric stiffness matrix
$K_{\phi\theta}$	= pyroelectric stiffness matrix
$K_{\phi\phi}$	= dielectric stiffness matrix
k	= stiffness constant
$k_{\theta\theta}$	= heat conduction stiffness matrix
L_u	= differential operator
N_u	= displacement shape function matrix
N_θ	= thermal shape function matrix
N_ϕ	= electric shape function matrix
P	= solution matrix to algebraic Riccati equation
$\boldsymbol{P}$	= vector of pyroelectric coefficients
Q	= positive semidefinite state weighting matrix
$\boldsymbol{Q}$	= global external heat vector
R	= positive definite input weighting matrix
$\boldsymbol{S}$	= strain vector
$\boldsymbol{T}$	= stress vector
$\boldsymbol{u}$	= global displacement vector
$\boldsymbol{u}_G$	= feedback voltage vector
$\dot{\boldsymbol{u}}$	= $\partial \boldsymbol{u}/\partial t$
$\ddot{\boldsymbol{u}}$	= $\partial^2 \boldsymbol{u}/\partial t^2$
V	= external electric voltage (potential)
W	= heat source intensity per unit volume per unit time
w	= deflection (transverse displacement)
w_t	= tip deflection
Y	= Young's modulus
$\boldsymbol{z}$	= state vector
α	= thermal expansion coefficient
α_R, β_R	= Rayleigh's proportional damping coefficients
ε	= matrix of dielectric coefficients
η	= entropy per unit volume
Θ	= absolute temperature
θ	= global temperature variation vector
θ_0	= reference temperature
λ	= vector of thermal expansion–stiffness coefficients
ρ	= mass density
ϕ	= global electric potential vector

I. Introduction

SENSING and control of distributed systems by piezoelectric materials have attracted many research activities in recent years.[1–3] Because of their distinct sensing and actuation nature, piezoelectric materials are ideally suited for the response sensing and monitoring of distributed systems. The piezoelectric materials are used by researchers in the sensing and control of such distributed systems as beams, plates, and shells.[4] Piezoelectric materials are bonded to surfaces of or embedded into the members of intelligent structures with highly sophisticated control architecture.[5]

The theory of piezoelectricity with inclusion of thermal field, thermopiezoelectricity, is well established in the literature. The governing equations of thermopiezoelectricity were first derived by Mindlin.[6] High-frequency motions of thermopiezoelectric crystal plates were studied by Mindlin.[7] General theorems of thermopiezoelectricity were used, and the general Hamilton's principle was obtained by Nowacki.[8]

The use of thermopiezoelectricity in the sensing and control of structural systems was presented recently by Rao and Sunar[9] to investigate the temperature effects in the sensing and control. It was shown that the temperature impact may be important when the piezoelectric sensing and control system is to operate in the environments where the temperature changes are of considerable magnitude. Thermal influences in the sensing and control of piezoelectric systems

Received Aug. 22, 1996; revision received Nov. 22, 1996; accepted for publication Nov. 25, 1996; also published in *AIAA Journal on Disc*, Volume 2, Number 2.

*Assistant Professor, Department of Mechanical Engineering.
†Professor, School of Mechanical Engineering, 1288 Mechanical Engineering Building. Member AIAA.

were also studied by Tzou and Ye.[10] General dynamic equations for thermopiezoelectric laminated plates were presented by Tang and Xu.[11] The delamination detection in thermal composite structures having piezoelectric layers was investigated by Birman et al.[12] by the use of thermopiezoelectricity and laminate theories.

The sensor and actuator placement is an important issue in the control area because the placement has an effect on the control efficiency and control cost. The issue of the piezoelectric sensor and actuator placement problem has been addressed recently by some researchers.[13,14] The same problem exists for the discretely placed piezoelectric sensors/actuators operating in the environments where the temperature effects are of considerable magnitude. This problem is named as thermopiezoelectric sensor/actuator placement or location problem in this work. The issue of the thermopiezoelectric sensor/actuator location problem appears to be lacking in the literature and needs to be addressed.

In this paper, the quasistatic thermopiezoelectricity equations are presented and used to develop the heat, sensor, and actuator equations. The generalized heat equation and Hamilton's principle, together with the finite element method (FEM), are used in formulating the equations. A robotic bimorph finger is taken as a static example to test the accuracy of the finite element development. A distributed control system consisting of a cantilever beam and a piezoelectric actuator pair covering the entire bottom and top surfaces of the beam is considered to further test the accuracy of the finite element approach and to observe the temperature effects in static and dynamic case studies. The thermopiezoelectric actuator location problem is considered on the same control system where the piezoelectric actuator pair only spans half the length of bottom and top surfaces of the beam. The thermopiezoelectric actuator location is varied on the two surfaces to see the effect of the change on the control efficiency. The thermal effect is assumed to be a uniformly elevated temperature field for this preliminary investigation.

II. Finite Element Formulation of Thermopiezoelectric Equations

The quasistatic thermopiezoelectricity equations are given by[7]

$$\boldsymbol{T} = c\boldsymbol{S} - e\boldsymbol{E} - \lambda\theta \qquad \boldsymbol{D} = e^T\boldsymbol{S} + \varepsilon\boldsymbol{E} + \boldsymbol{P}\theta$$
$$\eta = \lambda^T\boldsymbol{S} + \boldsymbol{P}^T\boldsymbol{E} + \alpha\theta \tag{1}$$

The following relations for the heat conduction and electric field are also noted[7]:

$$\boldsymbol{h} = -K\nabla\theta \qquad \boldsymbol{E} = -\nabla\phi \tag{2}$$

The generalized heat equation is written as

$$\Theta\dot{\eta} = -\nabla^T\boldsymbol{h} + W \tag{3}$$

where Θ is given as

$$\Theta = \theta_0 + \theta \tag{4}$$

For the finite element approximation of the heat equation, let

$$\boldsymbol{u}_{\mathrm{el}} = N_u\boldsymbol{u}_i \qquad \phi_{\mathrm{el}} = N_\phi\phi_i \qquad \theta_{\mathrm{el}} = N_\theta\theta_i \tag{5}$$

where $\boldsymbol{u}_{\mathrm{el}}$, $\boldsymbol{u}_i$, and N_u are the element and nodal displacement vectors and the shape function matrix for the displacement field, respectively, and so on. Using the preceding equations yields the finite element heat equation after the assemblage as

$$-C_{\theta u}\dot{\boldsymbol{u}} + C_{\theta\phi}\dot{\phi} - C_{\theta\theta}\dot{\theta} - K_{\theta\theta}\theta = \boldsymbol{Q} \tag{6}$$

The element matrices and external heat vector are found as

$$[C_{\theta u}]_{\mathrm{el}} = \int_{V_{\mathrm{el}}} \theta_0 N_\theta^T \lambda^T B_u\, dV \qquad [C_{\theta\phi}]_{\mathrm{el}} = \int_{V_{\mathrm{el}}} \theta_0 N_\theta^T \boldsymbol{P}^T B_\phi\, dV$$
$$[C_{\theta\theta}]_{\mathrm{el}} = \int_{V_{\mathrm{el}}} \theta_0 N_\theta^T \alpha N_\theta\, dV \qquad [K_{\theta\theta}]_{\mathrm{el}} = \int_{V_{\mathrm{el}}} B_\theta^T K^T B_\theta\, dV \tag{7}$$
$$\boldsymbol{Q}_{\mathrm{el}} = \int_{A_{\mathrm{el}}} N_\theta \boldsymbol{h}^T \boldsymbol{n}\, dA - \int_{V_{\mathrm{el}}} W N_\theta^T\, dV$$

where V_{el} is the element volume, A_{el} is the element area whose normal vector is $\boldsymbol{n}$, $B_u = L_u N_u$ with L_u denoting a differential operator matrix, $B_\phi = \nabla N_\phi$, and $B_\theta = \nabla N_\theta$.

To derive the actuator and sensor equations, a functional Π is defined as[8]

$$\Pi = \int_V (G + \eta\Theta)\, dV - \int_V \boldsymbol{u}^T\boldsymbol{P}_b\, dV$$
$$- \int_{S_1} \boldsymbol{u}^T\boldsymbol{P}_s\, dS - \boldsymbol{u}^T\boldsymbol{P}_c + \int_{S_2} \phi\sigma\, dS \tag{8}$$

where G is the thermopiezoelectric potential, $\boldsymbol{P}_b$ is the vector of body forces applied to volume V, $\boldsymbol{P}_s$ is the vector of surface forces applied to surface S_1, $\boldsymbol{P}_c$ is the vector of concentrated forces, and σ is the surface charge on surface S_2. Hamilton's principle is used to obtain the finite element formulation of the piezoelectric media. The principle is expressed as

$$\delta\int_{t_1}^{t_2} (T_k - \Pi)\, dt = 0 \tag{9}$$

where the kinetic energy T_k is given by

$$T_k = \frac{1}{2}\int_V \rho\dot{\boldsymbol{u}}^T\dot{\boldsymbol{u}}\, dV \tag{10}$$

where $\dot{\boldsymbol{u}}$ is the velocity vector. After writing the kinetic energy equation, one now writes Hamilton's principle, Eq. (9), as

$$\delta\int_{t_1}^{t_2} \Pi dt = \delta\int_{t_1}^{t_2} T_k\, dt = -\int_{t_1}^{t_2}\int_V \rho\delta\boldsymbol{u}^T\ddot{\boldsymbol{u}}\, dV\, dt \tag{11}$$

upon using integration by parts with proper boundary conditions. For the thermodynamic potential G,

$$\delta G = \delta\boldsymbol{S}^T\boldsymbol{T} - \delta\boldsymbol{E}^T\boldsymbol{D} - \delta\theta\eta \tag{12}$$

Using Eqs. (1), (9), (11), and (12) together with finite element equations (5) yields the actuator and sensor equations after the assemblage as

$$M_{uu}\ddot{\boldsymbol{u}} + K_{uu}\boldsymbol{u} + K_{u\phi}\phi - K_{u\theta}\theta = \boldsymbol{F}$$
$$K_{\phi u}\boldsymbol{u} - K_{\phi\phi}\phi + K_{\phi\theta}\theta = \boldsymbol{G} \tag{13}$$

The element matrices and vectors in Eq. (13) are found as

$$[M_{uu}]_{\mathrm{el}} = \int_{V_{\mathrm{el}}} \rho N_u^T N_u\, dV, \qquad [K_{uu}]_{\mathrm{el}} = \int_{V_{\mathrm{el}}} B_u^T c B_u\, dV$$
$$[K_{u\phi}]_{\mathrm{el}} = \int_{V_{\mathrm{el}}} B_u^T e B_\phi\, dV, \qquad [K_{u\theta}]_{\mathrm{el}} = \int_{V_{\mathrm{el}}} B_u^T \lambda N_\theta\, dV$$
$$[K_{\phi u}]_{\mathrm{el}} = \int_{V_{\mathrm{el}}} B_\phi^T e^T B_u\, dV, \qquad [K_{\phi\phi}]_{\mathrm{el}} = \int_{V_{\mathrm{el}}} B_\phi^T \varepsilon B_\Phi\, dV \tag{14}$$
$$[K_{\phi\theta}]_{\mathrm{el}} = \int_{V_{\mathrm{el}}} B_\phi^T \boldsymbol{P} N_\theta\, dV, \qquad G_{\mathrm{el}} = \int_{(S_2)_{\mathrm{el}}} N_\phi^T \sigma\, dS$$
$$F_{\mathrm{el}} = \int_{V_{\mathrm{el}}} N_u^T \boldsymbol{P}_b\, dV + \int_{(S_1)_{\mathrm{el}}} N_u^T \boldsymbol{P}_s\, dS + N_u^T \boldsymbol{P}_c$$

The heat, actuator, and sensor equations, Eqs. (6) and (13), can be collectively written as

$$\begin{bmatrix} M_{uu} & 0 & 0 \\ 0 & 0 & 0 \\ 0 & 0 & 0 \end{bmatrix}\begin{Bmatrix} \ddot{\boldsymbol{u}} \\ \ddot{\phi} \\ \ddot{\theta} \end{Bmatrix} + \begin{bmatrix} 0 & 0 & 0 \\ 0 & 0 & 0 \\ -C_{\theta u} & C_{\theta\phi} & -C_{\theta\theta} \end{bmatrix}\begin{Bmatrix} \dot{\boldsymbol{u}} \\ \dot{\phi} \\ \dot{\theta} \end{Bmatrix}$$
$$+ \begin{bmatrix} K_{uu} & K_{u\phi} & -K_{u\theta} \\ K_{\phi u} & -K_{\phi\phi} & K_{\phi\theta} \\ 0 & 0 & -K_{\theta\theta} \end{bmatrix}\begin{Bmatrix} \boldsymbol{u} \\ \phi \\ \theta \end{Bmatrix} = \begin{Bmatrix} \boldsymbol{F} \\ \boldsymbol{G} \\ \boldsymbol{Q} \end{Bmatrix} \tag{15}$$

Equation (15) can be used to study the temperature effects in distributed control systems with piezoelectric sensors and actuators. The temperature effects may be important if the control system has to operate in an environment where the impact of an existing thermal field cannot be neglected for the precision control.

III. Effect of Thermopiezoelectric Actuator Location on Control Performance

As stated before, due to their distinct characteristics, the piezoelectric materials are ideal to be employed in distributed sensing and control of systems. Piezoelectric actuators and sensors are major components of next-generation intelligent structures.

When the temperature effects are important, Eq. (15) can be used to include such effects. In the absence of temperature effects, Eq. (15) reduces to

$$\begin{bmatrix} M_{uu} & 0 \\ 0 & 0 \end{bmatrix} \begin{Bmatrix} \ddot{\boldsymbol{u}} \\ \ddot{\phi} \end{Bmatrix} + \begin{bmatrix} K_{uu} & K_{u\phi} \\ K_{\phi u} & -K_{\phi\phi} \end{bmatrix} \begin{Bmatrix} \boldsymbol{u} \\ \phi \end{Bmatrix} = \begin{Bmatrix} \boldsymbol{F} \\ \boldsymbol{G} \end{Bmatrix} \tag{16}$$

When a proportional damping term C_{uu} is added, Eq. (16) becomes

$$\begin{bmatrix} M_{uu} & 0 \\ 0 & 0 \end{bmatrix} \begin{Bmatrix} \ddot{\boldsymbol{u}} \\ \ddot{\phi} \end{Bmatrix} + \begin{bmatrix} C_{uu} & 0 \\ 0 & 0 \end{bmatrix} \begin{Bmatrix} \dot{\boldsymbol{u}} \\ \dot{\phi} \end{Bmatrix} + \begin{bmatrix} K_{uu} & K_{u\phi} \\ K_{\phi u} & -K_{\phi\phi} \end{bmatrix} \begin{Bmatrix} \boldsymbol{u} \\ \phi \end{Bmatrix} = \begin{Bmatrix} \boldsymbol{F} \\ \boldsymbol{G} \end{Bmatrix} \tag{17}$$

If the piezoelectric actuator pair does not cover the entire length of the surfaces of the beam, then the electric field in Eq. (17) changes, depending on the location of the actuator pair. The change in the electric field in turn affects the control performance of the system. To investigate the importance of temperature effects in the control performance when the actuator location is changed, it is assumed that the temperature of the system is homogeneously elevated. In other words, the temperature increase at some time, θ in Eq. (15), is assumed to be known for this preliminary investigation. Hence, Eq. (15) is written as

$$\begin{bmatrix} M_{uu} & 0 \\ 0 & 0 \end{bmatrix} \begin{Bmatrix} \ddot{\boldsymbol{u}} \\ \ddot{\phi} \end{Bmatrix} + \begin{bmatrix} C_{uu} & 0 \\ 0 & 0 \end{bmatrix} \begin{Bmatrix} \dot{\boldsymbol{u}} \\ \dot{\phi} \end{Bmatrix} + \begin{bmatrix} K_{uu} & K_{u\phi} \\ K_{\phi u} & -K_{\phi\phi} \end{bmatrix} \begin{Bmatrix} \boldsymbol{u} \\ \phi \end{Bmatrix} = \begin{Bmatrix} \boldsymbol{F} + K_{u\theta}\theta \\ \boldsymbol{G} - K_{\phi\theta}\theta \end{Bmatrix} \tag{18}$$

The linear quadratic regulator (LQR) method is used as the control scheme to investigate the change in control performance when the actuator pair location is varied. Equation (18) is converted to the standard state-space form as

$$\dot{\boldsymbol{z}} = A\boldsymbol{z} + B\boldsymbol{u}_G \tag{19}$$

The state vector $\boldsymbol{z}$ and matrix A and the input vector $\boldsymbol{u}_G$ and matrix B in Eq. (19) are written as

$$\boldsymbol{z} = \begin{Bmatrix} \boldsymbol{u} \\ \dot{\boldsymbol{u}} \end{Bmatrix}, \qquad \boldsymbol{u}_G = \frac{1}{c_p}\boldsymbol{G}$$

$$A = \begin{bmatrix} 0 & I \\ -M_{uu}^{-1}K^* & -M_{uu}^{-1}C_{uu} \end{bmatrix}, \qquad B = \begin{bmatrix} 0 \\ M_{uu}^{-1}D \end{bmatrix} \tag{20}$$

where

$$K^* = K_{uu} + K_{u\phi}K_{\phi\phi}^{-1}K_{\phi u}, \qquad D = c_p K_{u\phi}K_{\phi\phi}^{-1} \tag{21}$$

In Eq. (20), c_p is a constant and $\boldsymbol{u}_G$ is the feedback voltage vector chosen as

$$\boldsymbol{u}_G = -K_G\boldsymbol{z} \tag{22}$$

so that the performance index

$$J = \int_0^\infty (\boldsymbol{z}^T Q\boldsymbol{z} + \boldsymbol{u}_G^T R\boldsymbol{u}_G)\, dt \tag{23}$$

is minimized. In Eq. (23), Q and R are positive semidefinite and positive definite weighting matrices, respectively. The LQR scheme yields the constant gain matrix K_G to be

$$K_G = R^{-1}B^T P \tag{24}$$

where P is the solution matrix to the algebraic Riccati equation

$$PA + A^T P - PBR^{-1}B^T P + Q = 0 \tag{25}$$

After designing the controller using the LQR control scheme, we used Eq. (18) to study the effect of the thermopiezoelectric actuator placement on the control performance.

IV. Case Studies

Piezoelectric Bimorph Finger

A piezoelectric robotic bimorph finger[15] (Fig. 1) is used as a static example in case studies. Two layers of a piezoelectric film, polyvinylidene fluoride (PVDF), are bonded together to form a piezoelectric bimorph finger. The finger is modeled as a cantilever beam. The properties of PVDF at 300 and 350 K are given in Table 1. The poling directions for the two layers are opposite to each other, and hence a pure bending moment is obtained when an external voltage is applied to the layers. The dimensions of the finger are given as length $L = 100$ mm, height $h = 1$ mm, and depth = 5 mm.

The upper piezoelectric layer is subjected to a voltage of +250 V and the lower one to −250 V. In this case, the deflection of the finger (the transverse displacement w) can be theoretically found as[15]

$$w(x) = \frac{1.5e_{31}V}{Yh^2}x^2 \tag{26}$$

where e_{31} is the piezoelectric constant and V is the voltage difference between the upper and lower piezoelectric layers. When there are no temperature effects, the accuracy of the FEM results given in Fig. 2 can be easily verified by comparing them with the theoretical

Table 1 Properties of materials

	300 K	350 K
PVDF		
c_{11}, Pa	3.8×10^9	1.8×10^9
e_{31}, C/m^2	0.046	0.049
P_3, C/m^{2}K	4×10^{-5}	5.5×10^{-5}
K_{11}, W/mK	0.52	0.52
K_{33}, W/mK	0.12	0.12
ε_{11}, F/m	1.026×10^{-10}	1.553×10^{-10}
ε_{33}, F/m	1.026×10^{-10}	1.553×10^{-10}
α, 1/K	1.5×10^{-4}	2.15×10^{-4}
ρ, kg/m^3	1800	1800
c_p, F	3.8×10^{-6}	3.8×10^{-6}
Beam		
c_{11}, = Y, Pa	7.3×10^{10}	—
α, 1/K	2.4×10^{-5}	—
K_{11}, W/mK	248	—
ρ, kg/m^3	2750	—

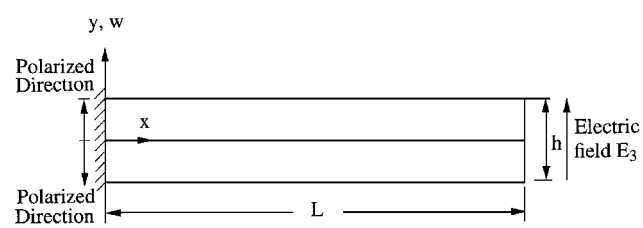

Fig. 1 Piezoelectric bimorph finger.

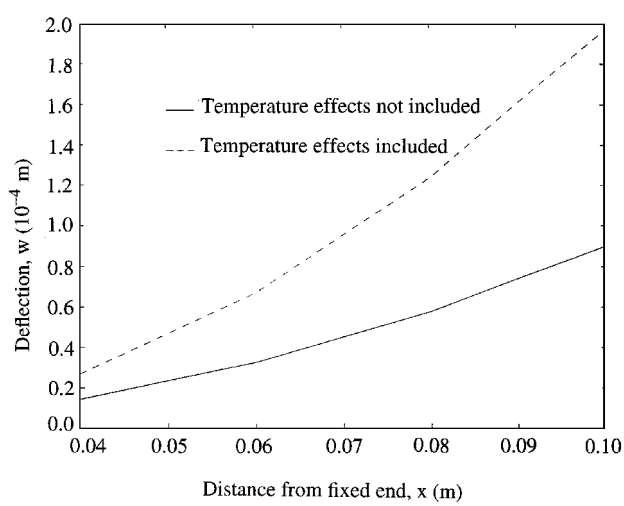

Fig. 2 Static deflection of the finger subjected to +250/−250 V potential.

results obtained using Eq. (26). As an example, at $x = L$ (at the tip of the finger), Eq. (26) results are $w(L) = 0.908 \times 10^{-4}$ m, which is comparable to the deflection value in Fig. 2.

To introduce temperature effects, it is assumed that the finger is heated such that a uniform temperature increase of 50 K from the room temperature, approximately 300 K, results, i.e., $\theta = 50$ K. When the finger is subjected to an electric voltage difference of 500 V under this temperature influence, the deflection curve is expected to be different, as shown in Fig. 2. The results plotted in Fig. 2 clearly indicate the impact of the thermal field in the deflection of the finger.

Distributed Control System

The distributed control system consisting of a cantilever beam and a piezoelectric actuator pair (Fig. 3) is used as a second example to observe the impact of the thermal field in static and dynamic response of the system. The beam is made up of aluminum whose material properties are given in Table 1. The height of the beam is taken as $h_b = 1$ cm and the piezoelectric layers as $h_p = 0.5$ mm. The length and depth of the control system are taken as $L = 0.5$ m and 1 cm, respectively. When there is no temperature field, the static deflection of the system to an electric potential of volts V at both upper and lower piezoelectric layers can be found as

$$w(x) = \frac{de_{31}(h_b + h_p)V}{2(Y_b I_b + Y_p I_p)} x^2 \tag{27}$$

where I_b and I_p denote moments of inertia for the beam and piezoelectric layers, respectively.

The static deflection of the control system when each piezoelectric actuator is subjected to an electric voltage of 500 V is shown in Fig. 4. The FEM results presented in Fig. 4 can be compared with the theoretical results of Eq. (27). For example, at $x = L$, Eq. (27) results in the deflection of $w(L) = 0.488 \times 10^{-5}$ m, which is comparable to the deflection value shown in Fig. 4.

Also shown in Fig. 4 is the static response of the system to the voltage of 500 V at both piezoelectric layers under the influence of a thermal field such that the temperature of the system is uniformly increased by 50 K from the room temperature. Thermal field can be seen to have introduced additional disturbance (deflection) into the system.

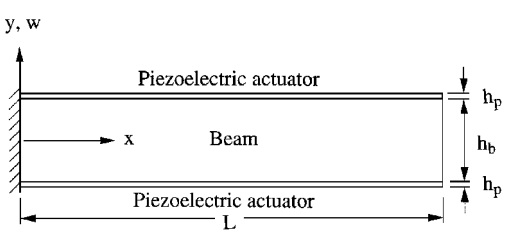

Fig. 3 Distributed piezoelectric/thermopiezoelectric control system.

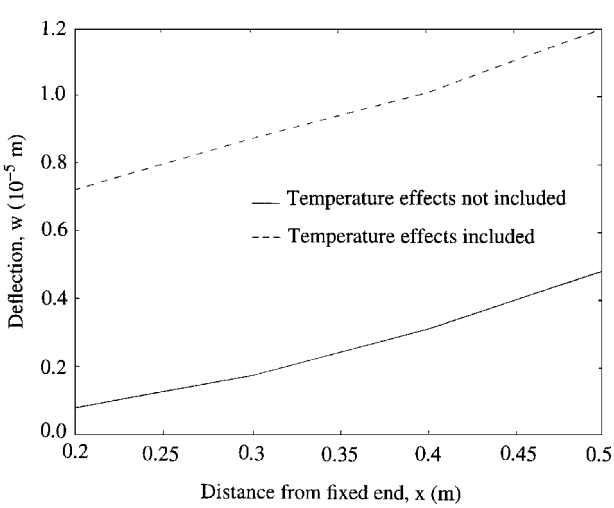

Fig. 4 Static deflection of the beam subjected to 500 V potential at both piezoelectric/thermopiezoelectric layers.

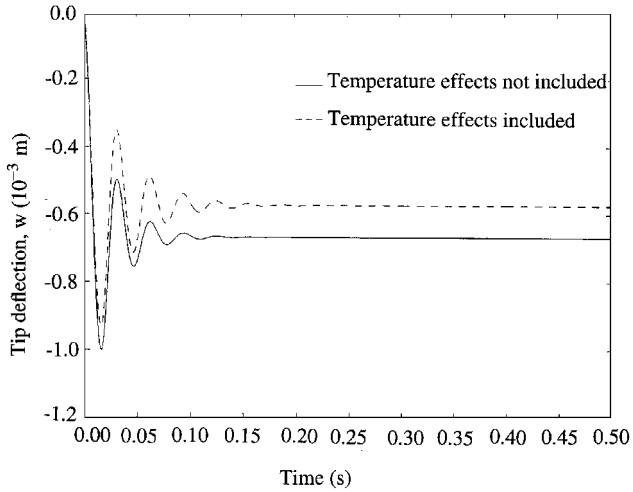

Fig. 5 Tip deflection of the closed-loop system due to a unit step force at the tip in $-y$ direction.

For the dynamic simulation of the control system, it is assumed that the system has proportional damping such that

$$C_{uu} = \alpha_R M_{uu} + \beta_R K_{uu} \tag{28}$$

where C_{uu} is the damping matrix. The Q and R matrices for the control design are chosen as $Q = 100 \times I_Q$ and $R = I_R$, where I_Q and I_R are identity matrices with same dimensions as Q and R, respectively. The tip deflection of the closed-loop system in response to a unit step force at the tip in the $-y$ direction is shown in Fig. 5.

The open-loop system can be approximately modeled as a one-degree-of-freedom (DOF) spring–mass system whose equation of motion without damping is simply given by

$$m\ddot{w}_t + kw_t = f \tag{29}$$

where m is the point mass (total mass of the system), k is the spring constant, and f is the external disturbance force. The spring constant k for this loading case is given as

$$k = k_b + k_p \tag{30}$$

where

$$k_b = \frac{3Y_b I_b}{L^3} \qquad k_p = \frac{3Y_p I_p}{L^3} \tag{31}$$

Equation (29) results in the steady-state tip deflection of the open-loop system as $w_t = w(L) = -1/k = -0.673 \times 10^{-3}$ m, which agrees well with the steady-state tip deflection of the system without temperature effects, as depicted in Fig. 5. Note that the controller has only a small effect on the steady-state value.

When the system is subjected to the same thermal field as in the previous cases, the response of the closed-loop system is different as shown in Fig. 5. The thermal field has introduced additional deflection in the closed-loop system, which is important to observe for the precision sensing and control. It also appears in Fig. 5 that the closed-loop system under temperature effects is slightly slower in the transient state.

Effect of Actuator Location on the Control Performance

The cantilever beam in the previous case is again taken as an example to investigate the effect of thermopiezoelectric actuator location on the control performance. In the present case, the actuator pair covers only half the length of bottom and top surfaces of the beam as shown in Fig. 6. The other dimensions of the system are the same as those in the previous example. The Q and R matrices of the LQR control scheme are also chosen to be the same as before. The distance of the actuator pair from the fixed end, d in Fig. 6, is varied to numerically observe its effect on the control performance with and without temperature influences. Because of the two-dimensional rectangular finite elements used, the lower and upper bounds imposed on d are taken as 0.05 and 0.15 m. Note

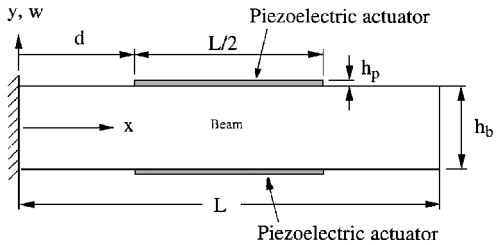

Fig. 6 Piezoelectric/thermopiezoelectric control system with actuator pair covering half the length.

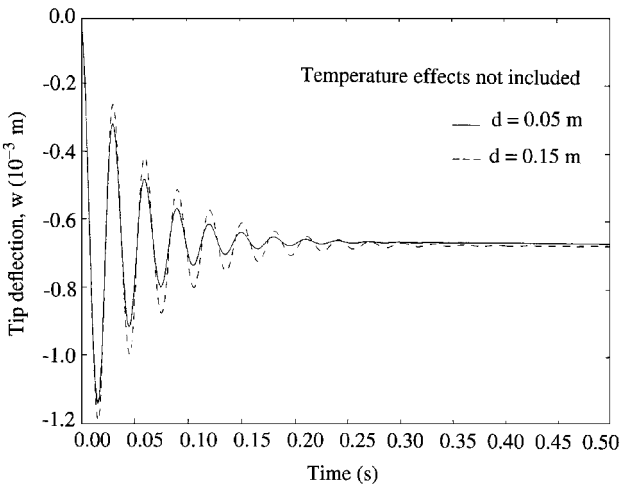

Fig. 7 Tip deflection of the closed-loop system due to a unit step force at the tip in $-y$ direction.

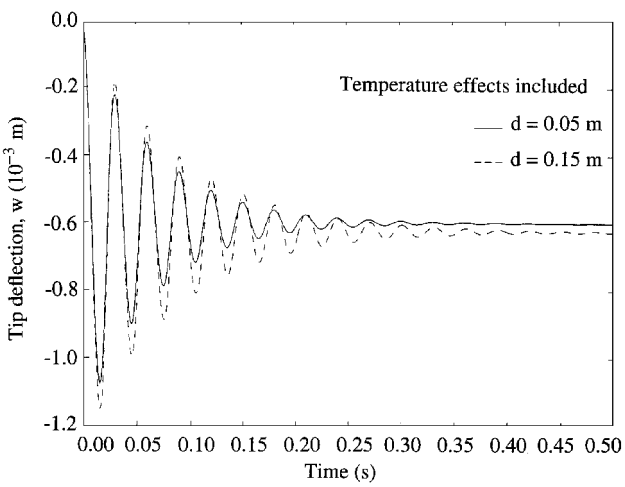

Fig. 8 Tip deflection of the closed-loop system due to a unit step force at the tip in $-y$ direction.

that the two-dimensional rectangular elements have pseudointernal DOF, which are well suited for vibrational problems.[16]

The tip deflections of the closed-loop system in response to a unit step force at the tip in the $-y$ direction are shown in Figs. 7–10. The actuator location has significant effects on the closed-loop characteristics such as settling time and maximum overshoot. It appears from the numerical results that the actuator pair that is closer to the fixed end results in less settling time and maximum overshoot as compared with the pair that is farther away from the fixed end. It can be observed that this trend is true with and without temperature effects. However, the temperature effects introduce additional steady-state deflection and more disturbance to the system.

The influence of including temperature effects on the location of actuators is studied by finding the absolute sum of the tip deflections of the beam from 0 to 0.5 s (depicted in Fig. 11). The sum of deflections is found by adding the absolute magnitudes of

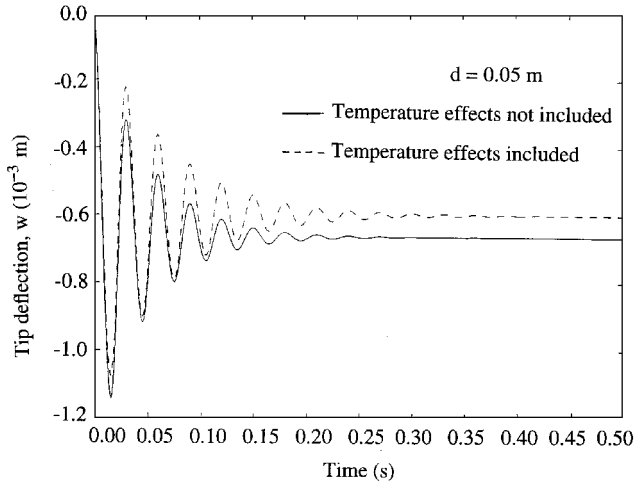

Fig. 9 Tip deflection of the closed-loop system due to a unit step force at the tip in $-y$ direction.

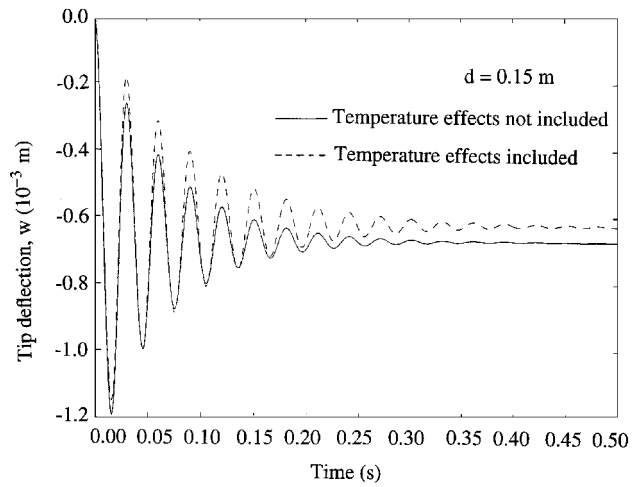

Fig. 10 Tip deflection of the closed-loop system due to a unit step force at the tip in $-y$ direction.

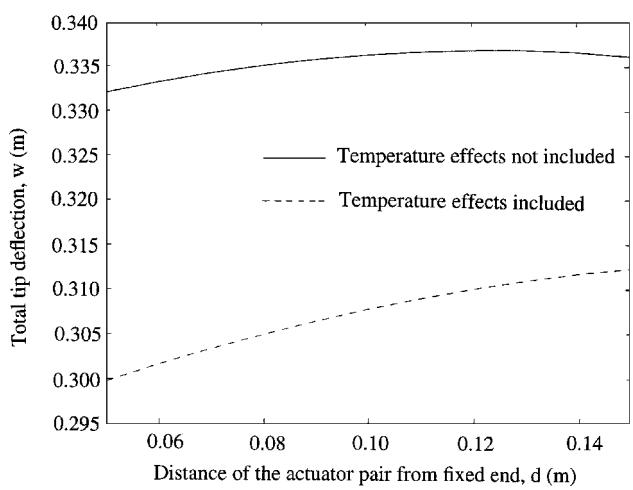

Fig. 11 Absolute sum of tip deflections of the closed-loop system from 0 to 0.5 s.

tip deflections at every 0.001 s from time 0 to 0.5 s. It is evident from the results in Fig. 11 that the actuator pair that is closer to the fixed end attenuates the oscillations faster, and hence it is more effective in this respect. Note that the thermal field introduces more deflections and the curve corresponding to the response with thermal field has steeper slope, indicating that the thermopiezoelectric actuator pair must be placed near the fixed end for a better control performance.

V. Conclusion

Thermopiezoelectric equations are presented for the distributed control systems. These equations are used for the finite element modeling of piezoelectric/thermopiezoelectric sensors and actuators. Finite element modeling includes the temperature effects, and hence it has the advantage of being an accurate model for the control cases where the temperature effects are important. It has been shown through numerical simulations and theoretical results that the finite element model developed in this work is accurate. Numerical results also show the importance of adding the temperature effects in the precision distributed control of systems.

The thermopiezoelectric actuator placement problem for the cantilever beamlike systems has also been presented. The inclusion of temperature has been observed to have the following effects: 1) an increase in the steady-state deflection and closed-loop response of the system for any specified location of the actuators, 2) an increase in the settling time and the maximum overshoot for a fixed location of the actuators, 3) an increase in the oscillatory behavior of the response when actuators are placed farther away from the fixed end, and 4) a steeper slope of the deflection curve of the closed-loop system with respect to the distance of the actuator from the fixed end. These observations lead to the conclusion that the actuators must be located as close to the fixed end as possible for a better structural control.

Acknowledgment

The first author acknowledges the support provided by King Fahd University of Petroleum and Minerals for this research.

References

[1]Hanagud, S., Obal, M. W., and Calise, A. J., "Optimal Vibration Control by the Use of Piezoceramic Sensors and Actautors," *Journal of Guidance, Control, and Dynamics*, Vol. 15, No. 5, 1992, pp. 1199–1206.

[2]Rao, S. S., and Sunar, M., "Piezoelectricity and Its Use in Disturbance Sensing and Control of Flexible Structures: A Survey," *Applied Mechanics Reviews*, Vol. 47, No. 4, 1994, pp. 113–123.

[3]Shen, M., and Herman, H., "Analysis of Beams Containing Piezoelectric Sensors and Actuators," *Smart Materials and Structures*, Vol. 3, No. 4, 1994, pp. 439–447.

[4]Gu, Y., Clark, R. L., Fuller, C. R., and Zander, A. C., "Experiments on Active Control of Plate Vibration Using Piezoelectric Actuators and Polyvinylidene Fluoride (PVDF) Modal Sensors," *Journal of Vibration and Acoustics*, Vol. 116, No. 3, 1994, pp. 303–308.

[5]Crawley, E. F., "Intelligent Structures for Aerospace: A Technology Overview and Assessment," *AIAA Journal*, Vol. 32, No. 8, 1994, pp. 1689–1699.

[6]Mindlin, R. D., "On the Equations of Motion of Piezoelectric Crystals," *Problems of Continuum Mechanics*, edited by J. Radok, Society for Industrial and Applied Mathematics, Philadelphia, PA, 1961, pp. 282–290.

[7]Mindlin, R. D., "Equations of High Frequency Vibrations of Thermopiezoelectric Crystal Plates," *International Journal of Solids and Structures*, Vol. 10, No. 6, 1974, pp. 625–637.

[8]Nowacki, W., "Some General Theorems of Thermopiezoelectricity," *Journal of Thermal Stresses*, Vol. 1, No. 2, 1978, pp. 171–182.

[9]Rao, S. S., and Sunar, M., "Analysis of Thermopiezoelectric Sensors and Actuators in Advanced Intelligent Structural Design," *AIAA Journal*, Vol. 31, No. 7, 1993, pp. 1280–1286.

[10]Tzou, H. S., and Ye, R., "Piezothermoelasticity and Precision Control of Piezoelectric Systems: Theory and Finite Element Analysis," *Journal of Vibration and Acoustics*, Vol. 116, Oct. 1994, pp. 489–495.

[11]Tang, Y. Y., and Xu, K., "Dynamic Analysis of a Piezothermoelastic Laminated Plate," *Journal of Thermal Stresses*, Vol. 18, No. 1, 1995, pp. 87–104.

[12]Birman, V., Saravanos, D. A., and Hopkins, D. A., "Sensory Composite Beams for Delamination Detection in Thermal Environments," *Adaptive Structures and Composite Materials: Analysis and Application*, Aerospace Div., AD 45, American Society of Mechanical Engineers, New York, 1994, pp. 351–358.

[13]Menon, R. G., Browder, A. M., Kurdila, A. J., and Junkins, J. L., "Concurrent Optimization of Piezoelectric Actuator Locations for Disturbance Attenuation," *AIAA/ASME/ASCE/AHS/ASC 34th Structures, Structural Dynamics, and Materials Conference* (La Jolla, CA), AIAA, Washington, DC, 1993, pp. 3269–3276.

[14]Chattopadhyay, A., and Seeley, C. E., "Multiobjective Design Optimization Procedure for Control of Structures Using Piezoelectric Materials," *Journal of Intelligent Material Systems and Structures*, Vol. 5, No. 3, 1994, pp. 403–411.

[15]Tzou, H. S., "Development of a Light-Weight Robot End-Effector Using Polymeric Piezoelectric Bimorph," *Proceedings of the 1989 IEEE International Conference on Robotics and Automation* (Scottsdale, AZ), Vol. 3, Inst. of Electrical and Electronics Engineers, Washington, DC, 1989, pp. 1704–1709.

[16]Tzou, H. S., and Tseng, C. I., "Distributed Piezoelectric Sensor/Actuator Design for Dynamic Measurement/Control of Distributed Parameter Systems: A Piezoelectric Finite Element Approach," *Journal of Sound and Vibration*, Vol. 137, No. 1, 1990, pp. 1–18.

R. K. Kapania
Associate Editor